MECHANICS
МЕХАНИКА

UDC 534.1, 539.3, 539.5
https://doi.org/10.23947/2687-1653-2026-26-1-2272

Original Theoretical Research

Applied Theory of Transverse Vibrations of Layered Structure with Polymer Matrices and Inclusions of Porous Piezoceramic Rods Arranged along the Layer

Arkadiy N. Soloviev[1,2] ✉, Maria S. Germanchuk [1,3], Pavel A. Oganesyan[4]

[1] Crimean Engineering and Pedagogical University named after Fevzi Yakubov, Simferopol, Republic of Crimea

[2] Research and Production Center for Engineering Technologies, Crimean Engineering and Pedagogical University named after Fevzi Yakubov, Simferopol, Republic of Crimea

[3] V.I. Vernadsky Crimean Federal University, Simferopol, Republic of Crimea

[4] Southern Federal University, Rostov-on-Don

✉ solovievarc@gmail.com

EDN: OLMHAS

Abstract

Introduction. The development of ultrasonic technology requires the creation of piezoelectric transducers with improved operational and metrological characteristics. One of the most promising directions is the use of composite materials. As shown in the literature, porous piezoceramics possess a unique property: their piezoelectric modulus d_{33} is practically independent of porosity, whereas the elastic moduli noticeably decrease as porosity increases. This opens up possibilities for the design of high-performance devices, particularly composites with a polymer matrix and porous piezoelectric ceramic rods with axial polarization. However, despite the sufficient study of their static properties, theoretical analysis of the dynamic behavior of such structures, including their simplified two-dimensional models, under bending vibrations and longitudinal polarization, is virtually absent in the scientific literature. In this regard, the objective of the work is to develop a simplified mathematical model for the analysis of bending vibrations of a layered plate of the specified composite and to identify the effect of porosity on its dynamic characteristics.

Materials and Methods. The structure is made of a piezoelectric composite consisting of several layers. Each layer is 1–3 piezoelectric composite, formed by a polymer matrix and porous longitudinally polarized piezoceramic rods. The mathematical formulation of the boundary value problems is performed within the framework of the linear theory of electroelasticity. Based on Kirchhoff-Love hypotheses and assumptions regarding the electric potential distribution, an applied method for calculating steady-state bending vibrations of a layered plate is proposed. The adequacy of the approach is verified through its comparison with the results of finite element modeling implemented in the ACELAN package.

Results. The key outcome of the study was the development and successful testing of an applied theory that reduced the three-dimensional boundary-value problem of electroelasticity for layered piezoelectric elements to a simpler two-dimensional formulation. This significantly reduced calculation time compared to traditional finite element methods while maintaining the required accuracy. To verify the proposed model, numerical testing was performed by comparing it with calculations in the ACELAN software package. The comparative analysis showed almost complete agreement between the results in the low-frequency range, including the precise determination of the first bending mode frequency. The obtained correspondence confirmed the high adequacy and reliability of the developed method, demonstrating its applicability as an efficient tool for the analysis and optimal design of piezoelectric devices.

Discussion. One of the key challenges in the design of layered piezoelectric transducers is the high resource intensity of three-dimensional modeling without transitioning to efficient characteristics, which significantly limits optimization possibilities. The proposed approach, based on reducing the three-dimensional problem to a two-dimensional one, represents a significant step forward in addressing this issue**.** Its main advantage is the reduction in computational costs

and the possibility of using simpler software tools compared to “heavy” CAE packages in numerical analysis. This opens the way to multiple runs, including those employing evolutionary algorithms, in the process of searching for the optimal geometry and structure of the piezoelectric element. Validation of the model based on comparison with calculations in the ACELAN finite element package has shown a high degree of correspondence in the low-frequency region, which confirms its adequacy for practical application. At the same time, the identified limitations related to the frequency range and differences in the elastic properties of the layers outline the boundaries of applicability and set directions for subsequent research.

Conclusion. As a result of the conducted research, an efficient calculation method has been developed and tested. It reduces the three-dimensional boundary value problem of electroelasticity for layered piezoelectric elements to a two-dimensional formulation. The main outcome is a significant acceleration of numerical modeling while maintaining accuracy. It is shown that the proposed theory provides high correctness of results in the low-frequency range, up to the first flexural mode, which has been confirmed by comparison with reference data from finite element analysis in ACELAN. This demonstrates the practical significance of the method as an efficient tool for the iterative search for the optimal design of converters. Prospects are opening up for its application in engineering practice when designing new types of piezoceramic devices, as well as for the further development of applied theory — in the direction of expanding the frequency range and adapting to more complex multilayer structures.

Keywords: composite materials, porous piezoceramics, layered plate, bending, applied theory, finite element method

Acknowledgements. The authors would like to thank the editorial board and reviewers for their attentive attitude towards the article.

Funding Information. The research is done with the financial support from RFFI (grant no. 22–11–00302 П) at the Southern Federal University. https://rscf.ru/project/22-11-00302/

For Citation. Soloviev AN, Germanchuk MS, Oganesyan PA. Applied Theory of Transverse Vibrations of Layered Structure with Polymer Matrices and Inclusions of Porous Piezoceramic Rods Arranged along the Layer. *Advanced Engineering Research (Rostov-on-Don).* 2026;26(1):2272. https://doi.org/10.23947/2687-1653-2026-26-1-2272

Оригинальное теоретическое исследование

Прикладная теория поперечных колебаний слоистой конструкции с полимерными матрицами и включениями из расположенных вдоль слоя пористых пьезокерамических стержней

А.Н. Соловьев[1,2] ✉, М.С. Германчук[1,3], П.А. Оганесян[4]

[1] Крымский инженерно-педагогический университет имени Февзи Якубова, г. Симферополь, Республика Крым

[2] Научно-производственный центр инжиниринговых технологий, Крымский инженерно-педагогический университет имени Февзи Якубова, г. Симферополь, Республика Крым

[3] Крымский федеральный университет им. В.И. Вернадского, г. Симферополь, Республика Крым

[4] Южный федеральный университет, г. Ростов-на-Дону, Российская Федерация

✉ solovievarc@gmail.com

Аннотация

Введение. Развитие ультразвуковой техники требует создания пьезоэлектрических преобразователей с улучшенными эксплуатационными и метрологическими характеристиками. Одним из наиболее перспективных направлений является применение композиционных материалов. Как показано в литературе, пористая пьезокерамика обладает уникальным свойством: ее пьезомодуль d_{33} практически не зависит от пористости, тогда как модули упругости заметно убывают при её увеличении. Это открывает возможности для проектирования высокоэффективных устройств, в частности композитов с полимерной матрицей и пористыми пьезокерамическими стержнями с осевой поляризацией. Однако, несмотря на достаточную изученность статических свойств, теоретический анализ динамического поведения таких структур, включая их упрощённые двумерные модели, при изгибных колебаниях и продольной поляризации в научной литературе практически отсутствует. В этой связи целью работы является разработка упрощённой математической модели для анализа изгибных колебаний слоистой пластины указанного композита и выявление влияния пористости на её динамические характеристики.

Материалы и методы. Материал конструкции — пьезоэлектрический композит, состоящий из нескольких слоёв. Каждый слой представляет собой пьезокомпозит связности 1–3, образованный полимерной матрицей и пористыми продольно поляризованными пьезокерамическими стержнями. Математическая постановка краевых задач выполнена в рамках линейной теории электроупругости. На основе гипотез типа Кирхгоффа-Лява и предположений о распределении электрического потенциала предложен прикладной метод расчёта установившихся изгибных колебаний слоистой пластины. Адекватность подхода проверена сопоставлением с результатами конечно-элементного моделирования, реализованного в пакете ACELAN.

Результаты исследования. Ключевым итогом работы стала разработка и успешная апробация прикладной теории, позволяющей свести трёхмерную краевую задачу электроупругости для слоистых пьезоэлементов к более простой двумерной постановке. Это обеспечило существенное сокращение времени расчёта по сравнению с традиционными методами конечных элементов при сохранении требуемой точности. Для верификации предложенной модели выполнено численное тестирование путём сравнения с расчётами в программном комплексе ACELAN. Сравнительный анализ показал практически полное совпадение результатов в низкочастотном диапазоне, включая точное определение частоты первой изгибной моды. Полученное соответствие подтверждает высокую адекватность и достоверность разработанного метода, демонстрируя его применимость в качестве эффективного инструмента для анализа и оптимального проектирования пьезоэлектрических устройств.

Обсуждение. Одной из ключевых проблем при проектировании слоистых пьезоэлектрических преобразователей является высокая ресурсоёмкость трёхмерного моделирования без перехода к эффективным характеристикам, что существенно ограничивает возможности оптимизации. Предложенный подход, основанный на сведении трёхмерной задачи к двумерной, представляет значимый шаг вперёд в решении этой проблемы. Его основное преимущество — снижение вычислительных затрат и возможность использования более простого программного инструментария по сравнению с «тяжёлыми» CAE-пакетами при численном анализе, что открывает путь к множественным прогонкам, в том числе с применением эволюционных алгоритмов, в процессе поиска оптимальной геометрии и структуры пьезоэлемента. Валидация модели на основе сравнения с расчётами в конечно-элементном пакете ACELAN показала высокую степень соответствия в низкочастотной области, что подтверждает её адекватность для практического применения. Вместе с тем выявленные ограничения, связанные с частотным диапазоном и различиями в упругих свойствах слоёв, очерчивают границы применимости и задают направления для последующих исследований.

Заключение. В результате проведённого исследования создан и апробирован эффективный метод расчёта, сводящий трёхмерную краевую задачу электроупругости для слоистых пьезоэлементов к двумерной постановке. Главный итог — существенное ускорение численного моделирования при сохранении точности. Показано, что предложенная теория обеспечивает высокую корректность результатов в низкочастотном диапазоне, вплоть до первой изгибной моды, что подтверждено сравнением с эталонными данными конечно-элементного анализа в ACELAN. Тем самым продемонстрирована практическая значимость метода как эффективного инструмента для итерационного поиска оптимальной конструкции преобразователей. Открываются перспективы его применения в инженерной практике при проектировании новых типов пьезокерамических устройств, а также для дальнейшего развития прикладной теории — в направлении расширения частотного диапазона и адаптации к более сложным многослойным структурам.

Ключевые слова: композитные материалы, пористая пьезокерамика, слоистая пластина, изгиб, прикладная теория, метод конечных элементов

Благодарности. Авторы выражают благодарность редакции журнала и рецензентам за внимательное отношение к статье.

Финансирование. Исследование выполнено при финансовой поддержке гранта РНФ (№ 22–11–00302 П) в Южном федеральном университете, https://rscf.ru/project/22-11-00302/

Для цитирования. Соловьев А.Н., Германчук М.С., Оганесян П.А. Прикладная теория поперечных колебаний слоистой конструкции с полимерными матрицами и включениями из расположенных вдоль слоя пористых пьезокерамических стержней. *Advanced Engineering Research (Rostov-on-Don).* 2026;26(1):2272. https://doi.org/10.23947/2687-1653-2026-26-1-2272

Introduction. To improve the efficiency of piezoelectric transducers, research is being conducted to find the optimal configuration of the device — its size, shape, electroplating pattern, loading methods, and the materials used. Despite a significant amount of work having been carried out, the task of determining efficient designs for piezoelectric generators and selecting piezo-materials with improved characteristics for energy storage devices remains a challenge. One of the

most promising ways to improve the performance of such transducers is the use of piezocomposite materials. The most well-known and thoroughly studied are fibrous piezocomposites, or systems with a 1–3 connectivity pattern according to Newnham's terminology [1], in which rod-shaped piezoceramic elements are embedded in an elastic dielectric matrix. Among numerous papers devoted to 1–3 composites, we should note [2], which examines applications for hydrophones. In [3], the efficient properties are calculated through solving boundary value problems by the finite element method for a unit cell with periodic boundary conditions. In [4], the corresponding coefficients are presented in closed form. In [5], formulas are derived based on asymptotic averaging, and comparison with experiment shows good agreement. Homogenization theory for the design of optimal piezocomposites is applied in [6]. In [7], analytical expressions for the effective constants are also obtained under the condition that the structure period is significantly smaller than the elastic wavelength, and new composites with improved global properties for biomedical imaging are proposed. An analysis of electroelastic composites using self-consistent methods and asymptotic homogenization is performed in [8]. In [9], a theoretical framework for designing piezocomposites with specified generalized characteristics is presented. Additional information is gathered in review [10]. 1–3 composites provide high values for a number of key parameters important for applications — the hydrostatic piezoelectric charge coefficient, the hydrostatic voltage coefficient, the thickness electromechanical coupling coefficient, the hydrostatic Q-factor, and others.

Macro fiber composites, originally developed for the aerospace industry, are also successfully used in energy harvesting systems. These miniature, low-power generators are thin beams and include piezoelectric fibers placed in a dielectric medium. The fibers are integrated into a single multilayer structure with interdigital electrodes on the lateral surfaces of the beams on both sides. The objective of [11] was to assess the effect of the uncertainty in the physical properties of both the piezoelectric fibers and the epoxy matrix on the model response, and to identify the parameters that determine the greatest variability in the output data. In [12], a potential technology is proposed for integrating energy harvesting sources into complex airframe structures in aerospace engineering, enabling the generation of the energy required for monitoring environmental conditions or controlled structural characteristics. A comparative analysis of generators made from monolithic and composite piezoceramics, conducted in [13], showed the high efficiency of using macro fiber composites. Study [14] presents the development of a microgenerator based on microcomposite piezoelectric materials for energy harvesting in glove structures. The devices described consist of piezoelectric fibers with a diameter of 90–250 μm, aligned in a unidirectional order and embedded in a composite structure.

To improve the performance of 1–3 composites, it is possible to vary the materials of the piezoelectric fibers and the elastic dielectric matrix. In particular, porous materials with a reduced Young's modulus and a significantly varying Poisson's ratio can be used as the matrix [2, 14]. In [15, 16], the Mori-Tanaka method is used to determine the effective moduli first for the porous matrix, after which an analysis of 1–3 composites is performed. In [15, 16], additional options for pore orientation relative to the polarization direction are considered, which, however, is difficult to implement in practice. In [2], approximations of the effective environmental method are used. In [17, 18] a topological optimization of the porous structure of the matrix is performed based on the approaches from [2]. In [19], a modeling of a 0–3 composite with piezoelectric particles in a porous matrix is performed. It is also shown that the use of a porous matrix does not lead to an improvement in the electromechanical properties of a 0–3 system. However, the piezoelectric sensitivity coefficients are not analyzed in that study.

Another direction of modification is related to the use of porous piezoceramics, which in recent years have been considered a promising active material for energy storage devices. Compared with dense ceramics, porous materials are characterized by reduced acoustic impedance, increased piezoelectric sensitivity, and a number of high-quality indicators. Thus, in [20], a Rosen-type piezoelectric element utilizing the longitudinal piezoelectric modulus is investigated. In [21], it is shown that introducing a porous layer into a multilayer element based on barium titanate significantly improves performance in piezoelectric energy harvesting. Experimental study [22] describes a piezoelectric generator manufactured using porous ceramics. In [23], a review of the current state and prospects for the use of porous piezoceramics is given.

The present study builds upon the results of [20, 24] and, to a certain extent, combines approaches to the introduction of porous piezoelectric ceramics as an active phase in 1–3 composite fibers and to varying matrix materials with different stiffness. In other words, it examines 1–3 piezoelectric composites in which porous piezoceramics are used as the piezoelectrically active material.

Thus, an analysis of the literature shows that the main efforts of researchers are focused on determining the efficient electroelastic properties of 1–3 composites. A wide range of methods has been developed — from analytical formulas to detailed numerical procedures — that make it possible to predict with high accuracy the homogenized (averaged) characteristics of the material depending on the properties of the constituent phases: the fibers and the matrix. This information is undoubtedly important, but it describes the behavior of the material as a whole, rather than that of the final structural element, which is the goal of engineering design.

The transition from efficient properties to the analysis of the dynamics of real structures, such as plates and shells, represents an independent and non-trivial problem. Although the finite element method (FEM) is applicable for high-precision analysis, as implemented in numerous software packages, full-scale three-dimensional modeling at the stages of preliminary design and optimization often proves to be excessively resource-intensive. At the same time, the development of applied two-dimensional theories (theories of plates and shells) that take into account the specific features of 1–3 composites (particularly in the presence of porous 3–0 and 3–3 components) would significantly simplify and speed up calculations, while maintaining accuracy sufficient for engineering applications. In the scientific literature, there is a distinct lack of such models capable of acting as a bridge between the micromechanics of the material and the macromechanics of the structure.

The objective of this work is to construct an applied two-dimensional theory for calculating the transverse vibrations of layered plates made of 1–3 piezoelectric composite, followed by validation of the results obtained using the proposed theory through comparing them with a solution from the ACELAN finite element package.

Materials and Methods. The development of a mathematical model based on the linear theory of electroelasticity and a computer model of a multilayer transducer with polarization along the layers is performed in the ACELAN finite element package. The computer model of the device is subsequently used to validate the adequacy of the developed applied theory.

Mathematical model

The paper considers models of piezoelectric transducers consisting of electroelastic composite materials, whose properties are specified by effective constants [20, 24]. Let us introduce index j for numbering the bodies and write down the equations and constitutive relations [25]:

$$\begin{gathered}\rho_j\omega^2\ddot{\mathbf{u}}+\alpha_j\rho_j\dot{\mathbf{u}}-\nabla\cdot\boldsymbol{\sigma}=f_j;\nabla\cdot\mathbf{D}=0;\\ \boldsymbol{\sigma}=\mathbf{c}_j^E\cdot\cdot(\boldsymbol{\varepsilon}+\beta_{dj}\dot{\boldsymbol{\varepsilon}})-\mathbf{e}_j^T\cdot\mathbf{E};\mathbf{E}=-\nabla\varphi;\\ \mathbf{D}+\varsigma_d\dot{\mathbf{D}}=\mathbf{e}_j\cdot\cdot(\boldsymbol{\varepsilon}+\varsigma_d\dot{\boldsymbol{\varepsilon}})+\mathfrak{e}_j^S\cdot\mathbf{E};\boldsymbol{\varepsilon}=(\nabla\mathbf{u}+\nabla\mathbf{u}^T)/2,\end{gathered}\tag{1}$$

where $\boldsymbol{\sigma}$ — stress tensor; ρ_j — density of the body; $\boldsymbol{\varepsilon}$ — strain tensor; $\mathbf{u}$ — displacement vector; $\mathbf{D}$ — electric induction vector; $\mathbf{E}$— electric field strength vector; $\mathbf{f}_j$ — vector of mass forces; φ — electric potential; α, β, ς, β_{dj}, ς_d — damping coefficients; $\mathbf{c}_j^E$, $\mathbf{e}_j^T$, $\mathfrak{e}_j^S$ — tensors of elastic constants, piezo moduli and permittivity; index j corresponds to the number of the body in the model.

System (1) is supplemented with the corresponding mechanical and electrical boundary conditions. In particular, the value of the electric potential φ is specified on the electrodes, and on the non-electrode part of the surface — the no-charge condition is set, i.e., the normal component of the electric induction vector $\mathbf{D}$ is equal to zero. In the case of free electrode S_E, potential V_0 on it is unknown and is determined from an additional condition:

$$\int_{S_E}\dot{D}_n\,ds=0.\tag{2}$$

The same condition is applied when determining the antiresonance frequencies.

To analyze the efficiency of the device, the values of the output electric potential, mechanical stresses, and the electromechanical coupling coefficient (EMCC) are used. This is calculated from the formula:

$$k=\sqrt{1-\left(f_r/f_a\right)^2},\tag{3}$$

where f_r and f_a — resonance and antiresonance frequencies, respectively.

The calculation of the damping coefficients when determining the output potential at resonant frequencies was performed using the approach from [25], for which a constant quality factor Q was assumed at the first two resonant frequencies:

$$\alpha_d=\frac{2\pi f_{r1}f_{r2}}{Q\left(f_{r1}+f_{r2}\right)},\quad \beta_d=\varsigma_d=\frac{1}{2\pi Q\left(f_{r1}+f_{r2}\right)}.\tag{4}$$

The operating frequencies (f_{r1}) and the next closest ones (f_{r2}) are selected as such resonant frequencies. For the structures under consideration, the operating frequency is the first bending mode.

When modeling porous composites, the efficient moduli obtained for porous PZT-4 piezoceramics by the averaging method [20, 26] in the ACELAN-COMPOS package were used. Data were obtained for materials with porosity up to 80%. The efficient moduli used in the numerical experiments are given in Table 1.

Table 1

Efficient Porous Ceramic Modules [20]

Porosity, %	0	10	20	30	40	50	60	70	80
ρ, kg/m^3	7500	6750	6000	5250	4500	3750	3000	2250	1500
c_{11}^E, GPa	139	115.6	92.5	68.5	50.5	33.4	20.7	12.6	6.8
c_{12}^E, GPa	77.8	61.5	46.6	31.4	21	11.6	6.2	2.8	1.3
c_{13}^E, GPa	74.3	58.2	42.5	28.2	18.7	10.6	5.2	2.4	1
c_{33}^E, GPa	115	95.3	72.3	54.2	39.1	27.2	16.3	9.1	4.7
c_{44}^E, GPa	25.6	22.3	18.3	14.4	11	7.4	4.4	2.3	1
e_{31}, C/m^2	–5.2	–4.23	–3.14	–2.07	–1.32	–0.75	–0.43	–0.21	–0.1
e_{33}, C/m^2	15.1	13.38	11.37	9.59	7.68	5.93	3.93	2.3	1.25
e_{15}, C/m^2	12.7	10.96	8.96	6.91	5	3.3	1.95	1	0.44
$\mathfrak{э}_{11}^S / \varepsilon_0$	730	663	582	509	439	349	263	191	122
$\mathfrak{э}_{33}^S / \varepsilon_0$	635	567	492	413	345	270	199	130	75

When modeling a 1–3 composite (Fig. 1), the effective properties (Tables 2, 3) are taken from [24].

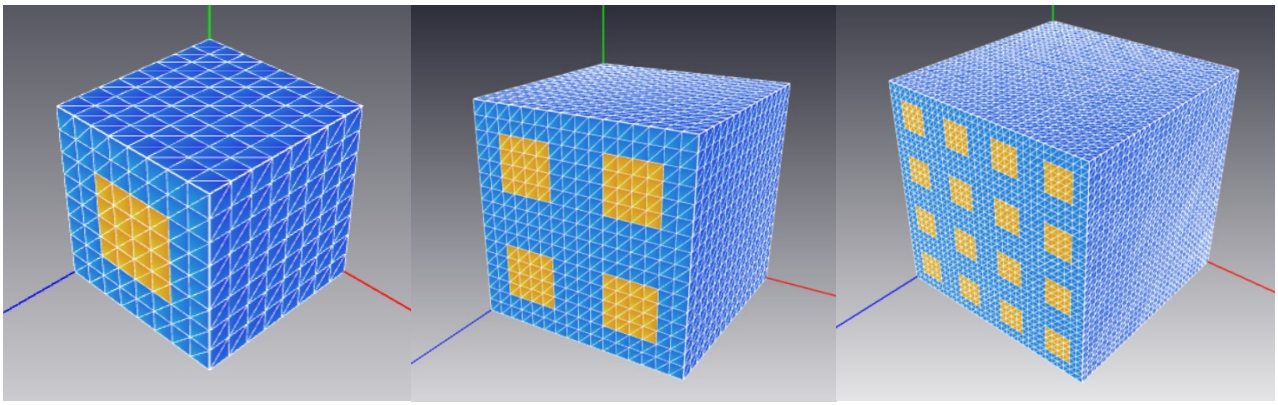

Fig. 1. Examples of representative 1–3 composite volumes, constructed in ACELAN-COMPOS complex

Table 2

Material Properties of Composite 1–3 with Matrix 1

Percentage of porosity	0	10	20	30	40	50	60	70	80
ρ, kg/m^3	5250	5060	4880	4690	4500	4310	4130	3940	3750
$c_{11}^{E\,\mathrm{eff}}$, 10^{10}, N/m^2	6.36	6.12	5.83	5.44	5.05	4.54	4.05	3.63	3.27
$c_{12}^{E\,\mathrm{eff}}$, 10^{10}, N/m^2	2.77	2.66	2.52	2.31	2.09	1.8	1.53	1.28	1.09
$c_{13}^{E\,\mathrm{eff}}$, 10^{10}, N/m^2	2.82	2.67	2.48	2.25	2.03	1.78	1.54	1.36	1.22
$c_{33}^{E\,\mathrm{eff}}$, 10^{10}, N/m^2	6.22	5.89	5.51	5.12	4.76	4.43	4.08	3.83	3.67
$c_{44}^{E\,\mathrm{eff}}$, 10^{10}, N/m^2	1.64	1.58	1.51	1.43	1.35	1.25	1.16	1.08	1.02
e_{33}^{eff}, C/m^2	–1.3	–1.05	–0.785	–0.523	–0.33	–0.185	–0.108	–0.053	–0.025
e_{31}^{eff}, C/m^2	3.77	3.35	2.86	2.4	1.93	1.49	0.972	0.58	0.31
e_{31}^{eff}, C/m^2	3.66	3.26	2.81	2.31	1.83	1.3	0.845	0.465	0.221
$\mathfrak{э}_{11}^{S\,\mathrm{eff}} / \varepsilon_0$	51.4	46.5	40.7	35.2	30.1	24.1	18.3	13.1	8.61
$\mathfrak{э}_{33}^{S\,\mathrm{eff}} / \varepsilon_0$	159	142	124	104	86.9	68.2	50.5	33.2	19.5

Table 3

Material Properties of Composite 1–3 with Matrix 2

Percentage of porosity	0	10	20	30	40	50	60	70	80
ρ, kg/m^3	3000	2810	2630	2440	2250	2060	1880	1690	1500
$c_{11}^{E\text{eff}}$, 10^{10}, N/m^2	1.15	1.13	1.1	1.06	1.02	0.956	0.882	0.796	0.685
$c_{12}^{E\text{eff}}$, 10^{10}, N/m^2	0.237	0.233	0.228	0.222	0.214	0.202	0.186	0.158	0.133
$c_{13}^{E\text{eff}}$, 10^{10}, N/m^2	0.332	0.315	0.294	0.269	0.246	0.219	0.184	0.155	0.125
$c_{33}^{E\text{eff}}$, 10^{10}, N/m^2	2.25	2.03	1.78	1.54	1.32	1.12	0.904	0.74	0.632
$c_{44}^{E\text{eff}}$, 10^{10}, N/m^2	0.425	0.415	0.403	0.388	0.369	0.341	0.304	0.261	0.219
e_{33}^{eff}, C/m^2	–1.3	–1.05	–0.785	–0.523	–0.33	–0.185	–0.108	–0.053	–0.025
e_{31}^{eff}, C/m^2	3.77	3.35	2.86	2.39	1.93	1.49	0.972	0.58	0.31
e_{31}^{eff}, C/m^2	1.44	1.35	1.24	1.1	0.959	0.783	0.591	0.381	0.209
$э_{11}^{S\text{eff}} / \varepsilon_0$	14.1	12.9	11.5	10.1	8.9	7.39	5.93	4.62	3.47
$э_{33}^{S\text{eff}} / \varepsilon_0$	159	142	123	104	86.9	68.2	50.5	33.2	19.5

Layered plate structures and finite element model

The piezoelectric element under consideration is a layered plate (Fig. 2), in which each layer is a 1–3 piezocomposite, with the piezoceramic rods (marked by black circles in Fig. 2) made of porous piezoceramics. It is noteworthy that two layers symmetric with respect to the midsurface have opposing longitudinal polarization.

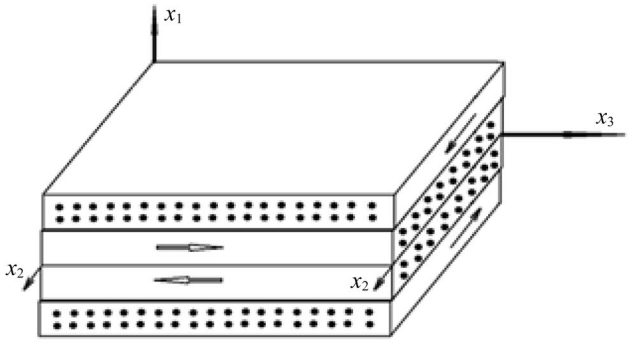

Fig. 2. Layered plate structures

In the case where the piezoelectric element consists of two layers, its finite element model is constructed. Figure 3 *a* presents the geometric model with two oppositely polarized layers (red and yellow colors), and Figure 3 *b* shows the mesh of triangular quadratic finite elements (1350 finite elements, 2839 nodes).

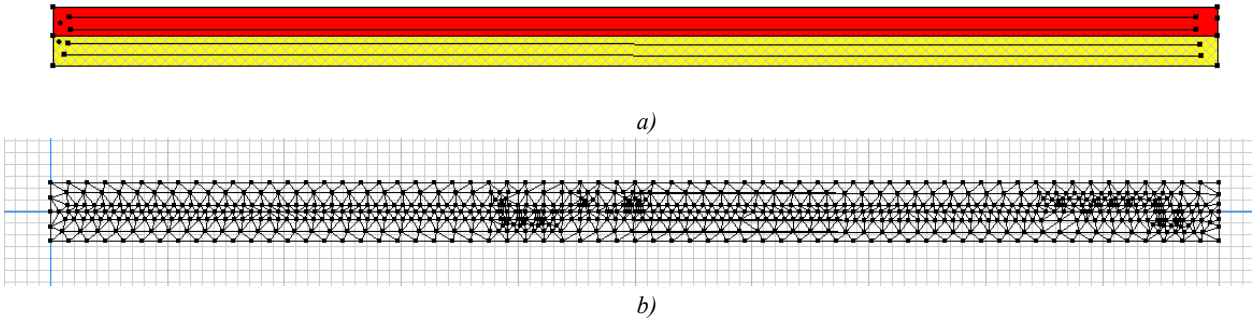

a)

b)

Fig. 3. Two-layer piezoelectric element: *a* — geometric model; *b* — finite element mesh

The finite element model constructed in this section was used to validate the adequacy of the applied theory in calculations in the following sections.

Research Results

Development of an applied theory for calculating transverse vibrations of a layered structure with polarization of layers in the plane of the plate

The applied theory of bending vibrations of the plate under consideration, consisting of four layers, in which the upper and lower layers are isotropic (thicknesses H with Lamé coefficients λ, μ), and the internal electroelastic thickness h is constructed on the basis of Kirchhoff-Love-type hypotheses. The first hypothesis is that normal stresses are equal to zero throughout the entire volume of the plate $\sigma_{11} = 0$, which makes it possible to express longitudinal deformations:

$$\varepsilon_{11} = -\frac{e_{31}\dfrac{\partial}{\partial z}\phi(x,y,z) + c_{12}\varepsilon_{22} + c_{13}\varepsilon_{33}}{c_{11}}. \tag{5}$$

The second hypothesis shows that the distribution of the components of the displacement vector and the electric potential has the form:

$$\begin{gathered} u_1(x,y,z) = UX(y,z),\ u_2(x,y,z) = -\left(\frac{\partial}{\partial y}UX(y,z)\right)x,\ u_3(x,y,z) = -\left(\frac{\partial}{\partial z}UX(y,z)\right)x, \\ \phi(x,y,z) = \Phi(y,z),\ \varepsilon_{22} = -\left(\frac{\partial^2}{\partial y^2}UX(y,z)\right)x,\ \varepsilon_{33} = -\left(\frac{\partial^2}{\partial z^2}UX(y,z)\right)x, \end{gathered} \tag{6}$$

where $UX(y, z)$ — deflection of the midsurface, $x_1 = x$, $x_2 = y$, $x_3 = z$.

Taking into account relations (5) and (6) in system (1) in the case of steady-state vibrations with circular frequency ω leads to a system of equations for two unknown functions $\Phi(y, z)$, $UX(y, z)$.

$$\begin{gathered} \left(-\frac{1}{2}\left(2e_{31} - \frac{2c_{12}e_{31}}{c_{11}}\right)\left(\left(\frac{1}{2}h+H\right)^2 - \frac{1}{4}h^2\right) - 2e_{15}\left(\left(\frac{1}{2}h+H\right)^2 - \frac{1}{4}h^2\right)\right)\times \\ \times\left(\frac{\partial^3}{\partial z\partial y^2}\Phi(y,z)\right) - \frac{1}{2}\left(-\frac{2c_{13}e_{31}}{c_{11}} + 2e_{33}\right)\left(\left(\frac{1}{2}h+H\right)^2 - \frac{1}{4}h^2\right)\times \\ \times\left(\frac{\partial^3}{\partial z\partial y^2}\Phi(y,z)\right) - \frac{1}{2}\left(-\frac{2c_{13}e_{31}}{c_{11}} + 2e_{33}\right)\left(\left(\frac{1}{2}h+H\right)^2 - \frac{1}{4}h^2\right)\left(\frac{\partial^3}{\partial z^3}\Phi(y,z)\right) + \\ + \left(-\frac{1}{3}\left(\frac{2c_{12}^2}{c_{11}} - 2c_{11}\right)\left(\left(\frac{1}{2}h+H\right)^3 - \frac{1}{8}h^3\right) - \frac{1}{24}\left(-2\lambda - 4\mu + \frac{2\lambda^2}{\lambda+2\mu}\right)h^3\right)\times \\ \times\left(\frac{\partial^4}{\partial y^4}UX(y,z)\right) + \left(\frac{1}{3}\mu h^3 + \frac{8}{3}c_{44}\left(\left(\frac{1}{2}h+H\right)^3\right) - \frac{1}{8}h^3\right) - \frac{2}{3}\left(\frac{2c_{12}c_{13}}{c_{11}} - 2c_{13}\right)\times \\ \times\left(\left(\frac{1}{2}h+H\right)^3 - \frac{1}{8}h^3\right) - \frac{1}{12}\left(\frac{2\lambda^2}{\lambda+2\mu} - 2\lambda\right)h^3\left(\frac{\partial^4}{\partial z^2\partial y^2}UX(y,z)\right) + \\ + \left(-\frac{1}{3}\left(\frac{2c_{13}^2}{c_{11}} - 2c_{33}\right)\left(\left(\frac{1}{2}h+H\right)^3 - \frac{1}{8}h^3\right) - \frac{1}{24}\left(-2\lambda - 4\mu + \frac{2\lambda^2}{\lambda+2\mu}\right)h^3\right)\times \\ \times\left(\frac{\partial^4}{\partial z^4}UX(y,z)\right) - \omega^2\rho h UX(y,z) - p(y,z) = 0. \\ -2g_{11}\left(\frac{\partial^2}{\partial y^2}\Phi(y,z)\right) + \left(-\frac{2e_{31}^2}{c_{11}} - 2g_{33}\right)\left(\frac{\partial^2}{\partial z^2}\Phi(y,z)\right) + \\ + \frac{1}{H}\left(\left(\frac{c_{12}e_{31}}{c_{11}} - 2e_{15} - e_{31}\right)\left(\left(\frac{1}{2}h+H\right)^2 - \frac{1}{4}h^2\right)\left(\frac{\partial^3}{\partial z\partial y^2}UX(y,z)\right)\right) + \\ + \frac{1}{H}\left(\left(\frac{c_{13}e_{31}}{c_{11}} - e_{33}\right)\left(\left(\frac{1}{2}h+H\right)^2 - \frac{1}{4}h^2\right)\left(\frac{\partial^3}{\partial z^3}UX(y,z)\right)\right) = 0. \end{gathered} \tag{7}$$

Bending moments and shear forces have the form:

$$M_{22}=\frac{1}{24}\left(-2(\lambda+2\mu)\left(\frac{\partial^2}{\partial y^2}UX(y,z)\right)-\right.$$
$$-\frac{1}{\lambda+2\mu}\left(2\lambda\left(-\left(\frac{\partial^2}{\partial y^2}UX(y,z)\right)\lambda-\lambda\left(\frac{\partial^2}{\partial z^2}UX(y,z)\right)\right)\right)-2\lambda\left(\frac{\partial^2}{\partial z^2}UX(y,z)\right)\Bigg)\times$$
$$-2c_{13}\left(\frac{\partial^2}{\partial z^2}UX(y,z)\right)-2c_{11}\left(\frac{\partial^2}{\partial y^2}UX(y,z)\right)\Bigg)\left(\left(\frac{1}{2}h+H\right)^3-\frac{1}{8}h^3\right)+$$
$$+\frac{1}{2}\left(2e_{31}\left(\frac{\partial}{\partial z}\Phi(y,z)\right)-\frac{2c_{12}e_{31}\left(\frac{\partial}{\partial z}\Phi(y,z)\right)}{c_{11}}\right)\left(\left(\frac{1}{2}h+H\right)^2-\frac{1}{4}h^2\right).$$

$$M_{33}=\frac{1}{24}\left(-\frac{1}{\lambda+2\mu}\left(2\lambda\left(-\left(\frac{\partial^2}{\partial y^2}UX(y,z)\right)\lambda-\lambda\left(\frac{\partial^2}{\partial z^2}UX(y,z)\right)\right)\right)-\right.$$
$$-2\left(\frac{\partial^2}{\partial y^2}UX(y,z)\right)\lambda-2(\lambda+2\mu)\left(\frac{\partial^2}{\partial z^2}UX(y,z)\right)\Bigg)h^3+$$
$$+\frac{1}{3}\left(-\frac{1}{c_{11}}\left(2c_{13}\left(-\left(\frac{\partial^2}{\partial y^2}UX(y,z)\right)c_{12}-c_{13}\left(\frac{\partial^2}{\partial z^2}UX(y,z)\right)\right)\right)-\right.$$
$$-2c_{13}\left(\frac{\partial^2}{\partial y^2}UX(y,z)\right)-2c_{33}\left(\frac{\partial^2}{\partial z^2}UX(y,z)\right)\Bigg)\left(\left(\frac{1}{2}h+H\right)^3-\frac{1}{8}h^3\right)+$$
$$+\frac{1}{2}\left(-\frac{2c_{13}e_{31}\left(\frac{\partial}{\partial z}\Phi(y,z)\right)}{c_{11}}+2e_{33}\left(\frac{\partial}{\partial z}\Phi(y,z)\right)\right)\left(\left(\frac{1}{2}h+H\right)^2-\frac{1}{4}h^2\right).$$

$$M_{23}=-\frac{1}{6}\mu\left(\frac{\partial^2}{\partial z\partial y}UX(y,z)\right)h^3-\frac{4}{3}\left(\frac{\partial^2}{\partial z\partial y}UX(y,z)\right)c_{44}\left(\left(\frac{1}{2}h+H\right)^3-\frac{1}{8}h^3\right)+$$
$$+e_{15}\left(\frac{\partial}{\partial y}\Phi(y,z)\right)\left(\left(\frac{1}{2}h+H\right)^2-\frac{1}{4}h^2\right).$$

$$Q_2=\frac{1}{6}\mu\left(\frac{\partial^3}{\partial z^2\partial y}UX(y,z)\right)h^3+\frac{4}{3}\left(\frac{\partial^3}{\partial z^2\partial y}UX(y,z)\right)c_{44}\left(\left(\frac{1}{2}h+H\right)^3-\frac{1}{8}h^3\right)-$$
$$-e_{15}\left(\frac{\partial^2}{\partial z\partial y}\Phi(y,z)\right)\left(\left(\frac{1}{2}h+H\right)^2-\frac{1}{4}h^2\right)-\frac{1}{24}\left(-2(\lambda+2\mu)\left(\frac{\partial^3}{\partial y^3}UX(y,z)\right)-\right.$$
$$-\frac{1}{\lambda+2\mu}\left(2\lambda\left(-\left(\frac{\partial^3}{\partial y^3}UX(y,z)\right)\lambda-\lambda\left(\frac{\partial^3}{\partial z^2\partial y}UX(y,z)\right)\right)\right)-2\lambda\left(\frac{\partial^3}{\partial z^2\partial y}UX(y,z)\right)\Bigg)h^3-$$
$$-\frac{1}{3}\left(-\frac{1}{c_{11}}\left(2c_{12}\left(-\left(\frac{\partial^3}{\partial y^3}UX(y,z)\right)c_{12}-c_{13}\left(\frac{\partial^3}{\partial z^2\partial y}UX(y,z)\right)\right)\right)-\right.$$
$$-2c_{13}\left(\frac{\partial^3}{\partial z^2\partial y}UX(y,z)\right)-2c_{11}\left(\frac{\partial^3}{\partial y^3}UX(y,z)\right)\Bigg)\left(\left(\frac{1}{2}h+H\right)^3-\frac{1}{8}h^3\right)-$$
$$-\frac{1}{2}\left(2e_{31}\left(\frac{\partial^2}{\partial z\partial y}\Phi(y,z)\right)-\frac{2c_{12}e_{31}\left(\frac{\partial^2}{\partial z\partial y}\Phi(y,z)\right)}{c_{11}}\right)\left(\left(\frac{1}{2}h=H\right)^2-\frac{1}{4}h^2\right).$$

$$Q_3 = -\frac{1}{24}\left(-\frac{1}{\lambda+2\mu}\left(2\lambda\left(-\left(\frac{\partial^3}{\partial z\partial y^2}UX(y,z)\right)\lambda-\lambda\left(\frac{\partial^3}{\partial z^3}UX(y,z)\right)\right)\right)-\right.$$
$$\left.-2\left(\frac{\partial^3}{\partial z\partial y^2}UX(y,z)\right)\lambda-2(\lambda+2\mu)\left(\frac{\partial^3}{\partial z^3}UX(y,z)\right)\right)h^3-$$
$$-\frac{1}{3}\left(-\frac{1}{c_{11}}\left(2c_{13}\left(-\left(\frac{\partial^3}{\partial z\partial y^2}UX(y,z)\right)c_{12}-c_{13}\left(\frac{\partial^3}{\partial z^3}UX(y,z)\right)\right)\right)-\right.$$
$$\left.-2c_{13}\left(\frac{\partial^3}{\partial z\partial y^2}UX(y,z)\right)-2c_{33}\left(\frac{\partial^3}{\partial z^3}UX(y,z)\right)\right)\left(\left(\frac{1}{2}h+H\right)^3-\frac{1}{8}h^3\right)-$$
$$-\frac{1}{2}\left(-\frac{2c_{13}e_{31}\left(\frac{\partial^2}{\partial z^2}\Phi(y,z)\right)}{c_{11}}+2e_{33}\left(\frac{\partial^2}{\partial z^2}\Phi(y,z)\right)\right)\left(\left(\frac{1}{2}h+H\right)^2-\frac{1}{4}h^2\right)+$$
$$+\frac{1}{6}\mu\left(\frac{\partial^3}{\partial z\partial y^2}UX(y,z)\right)h^3+\frac{4}{3}\left(\frac{\partial^3}{\partial z\partial y^2}UX(y,z)\right)c_{44}\left(\left(\frac{1}{2}h+H\right)^3-\frac{1}{8}h^3\right)-$$
$$-e_{15}\left(\frac{\partial^2}{\partial y^2}\Phi(y,z)\right)\left(\left(\frac{1}{2}h+H\right)^2-\frac{1}{4}h^2\right).$$

For the case of a panel consisting of two internal layers (Fig. 2 and 3 *a*), the second equation of system (7) is reduced to the form:

$$\frac{1}{4}\left(\frac{c_{13}e_{31}}{c_{11}}-e_{33}\right)h\left(\frac{d}{dz}UX(z)\right)+\left(-\frac{e_{31}^2}{c_{11}}-g_{33}\right)\Phi(z)+C_1z+C_2=0, \tag{8}$$

from which the electric potential is expressed:

$$\Phi(z)=\frac{1}{4}\frac{\left(-c_{11}e_{33}h+c_{13}e_{31}h\right)\left(\frac{d}{dz}UX(z)\right)}{g_{33}c_{11}+e_{31}^2}+\frac{1}{4}\frac{4C_1c_{11}z+4C_2c_{11}}{g_{33}c_{11}+e_{31}^2}. \tag{9}$$

After this, the first equation (7) is reduced to the form:

$$\left(-\frac{1}{24}\left(\frac{2c_{13}^2}{c_{11}}-2c_{33}\right)h^3-\frac{1}{32}\frac{1}{c_{11}g_{33}+e_{31}^2}\left(\left(-\frac{2c_{13}e_{31}}{c_{11}}+2e_{33}\right)h^2\left(-c_{11}e_{33}h+c_{13}e_{31}h\right)\right)\right)\times$$
$$\times\left(\frac{d^4}{dz^4}UX(z)\right)-\omega^2\rho hUX(z)-p(z)=0. \tag{10}$$

System of equations (7) is generally solved numerically, whereas equation (10) can be solved analytically.

Validation of the proposed method for adequacy based on a comparison of the results with calculations in the ACELAN package

To test the applicability of the proposed applied theory, two problems for a two-layer panel are solved: determining the first resonant frequency of the bending mode, and the problem of steady-state vibrations at a frequency of 200 Hz under a uniformly distributed load on the upper plane of the plate with an amplitude of 1000 Pa. The plate length is 0.1 m, the thickness of each layer is 0.0025 m, and the material is PZT-4. The plate is fixed at the left end and hinged at the right (Fig. 3 *a*).

The self-resonant frequency of the first bending mode (Fig. 4) in the ACELAN package calculation is 1348.68 Hz, while the applied theory calculation is 1360 Hz, i.e., the error is 0.8%.

The forced vibration calculation has yielded the following results: Figure 4 shows the distribution of vertical displacements on the deformed plate.

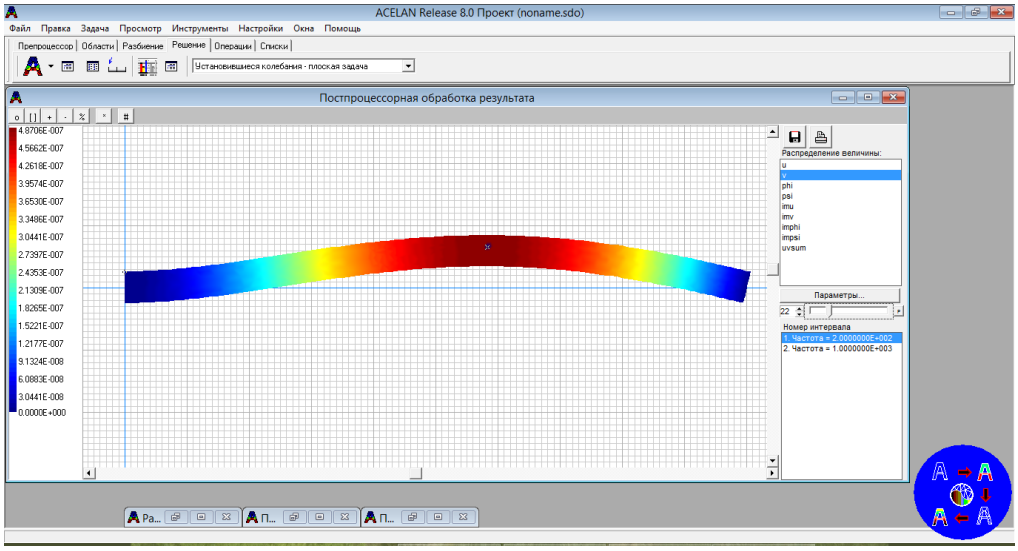

Fig. 4. Distribution of vertical displacement at a frequency of 200 Hz

Figure 5 shows the graphs of the deflection of the midsurface of the plate.

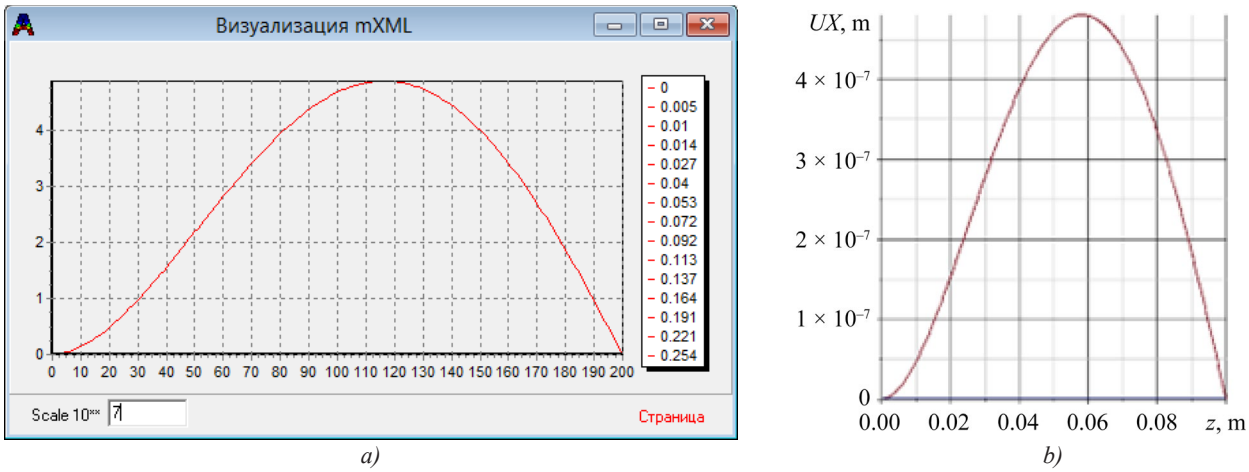

a) *b)*

Fig. 5. Plate deflection: *a* — ACELAN; *b* — applied theory of equation (8)–(10)

Figures 6 and 7 present similar results for horizontal displacement, and Figures 8 and 9 show them for electric potential.

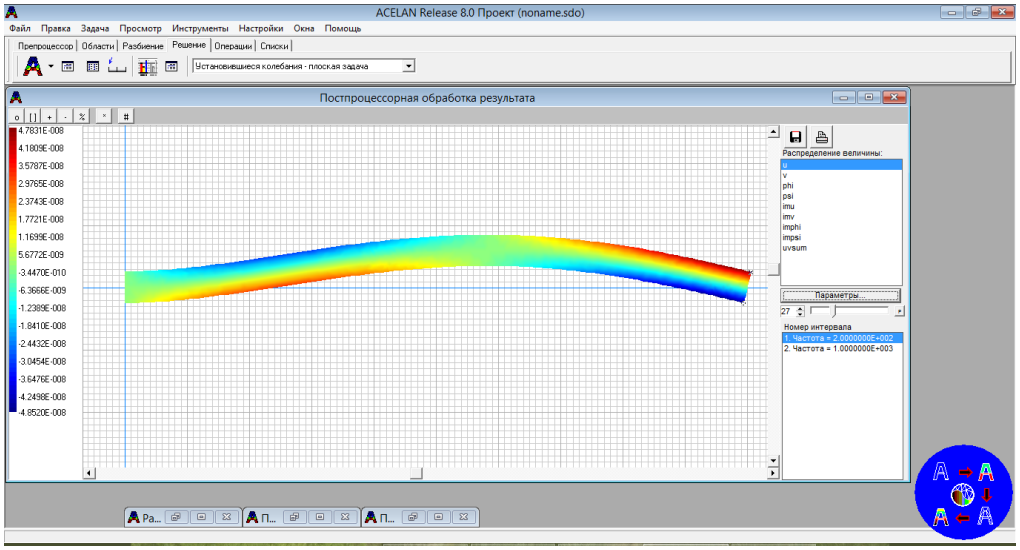

Fig. 6. Distribution of horizontal displacement at a frequency of 200 Hz

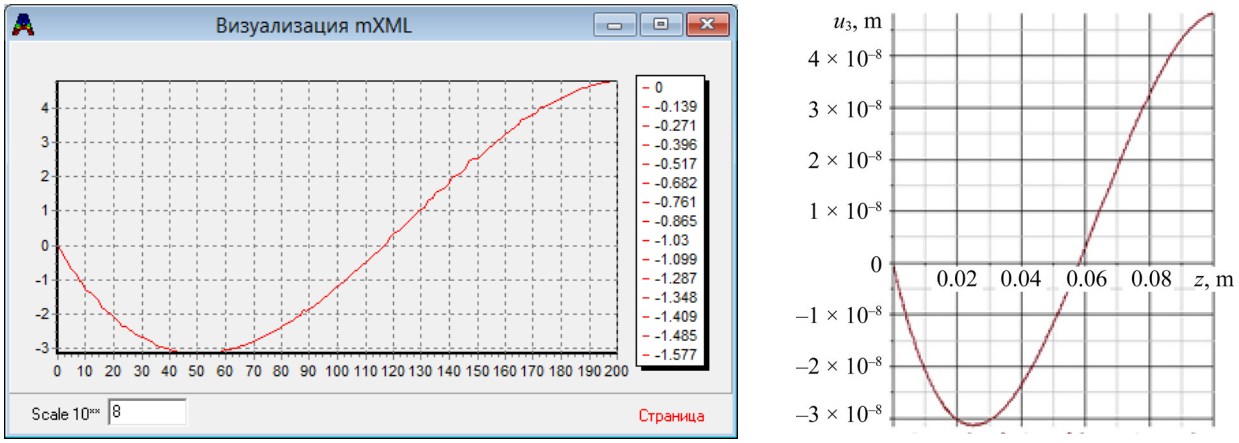

a) *b)*

Fig. 7. Horizontal displacement on the plate surface:
a — ACELAN; *b* — applied theory

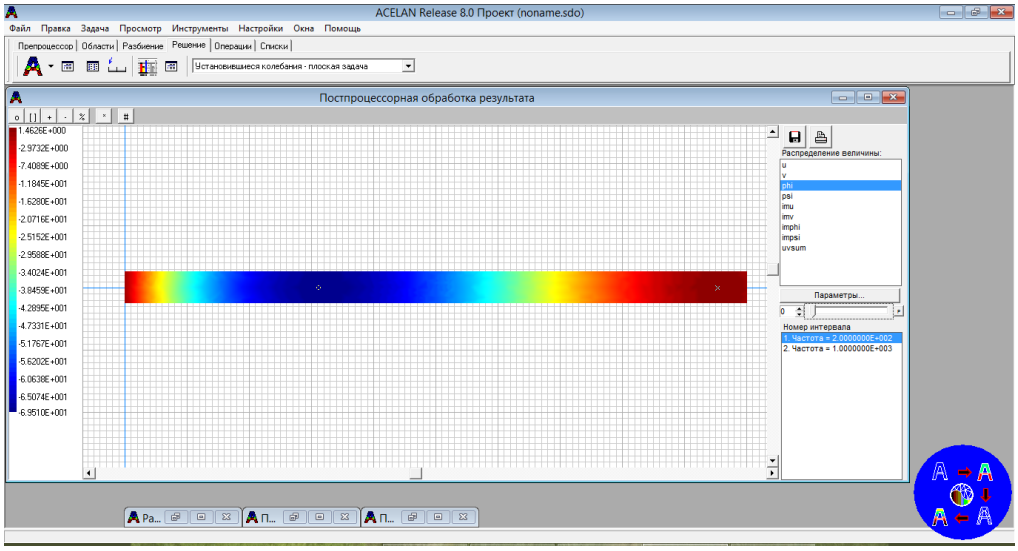

Fig. 8. Distribution of electric potential at a frequency of 200 Hz

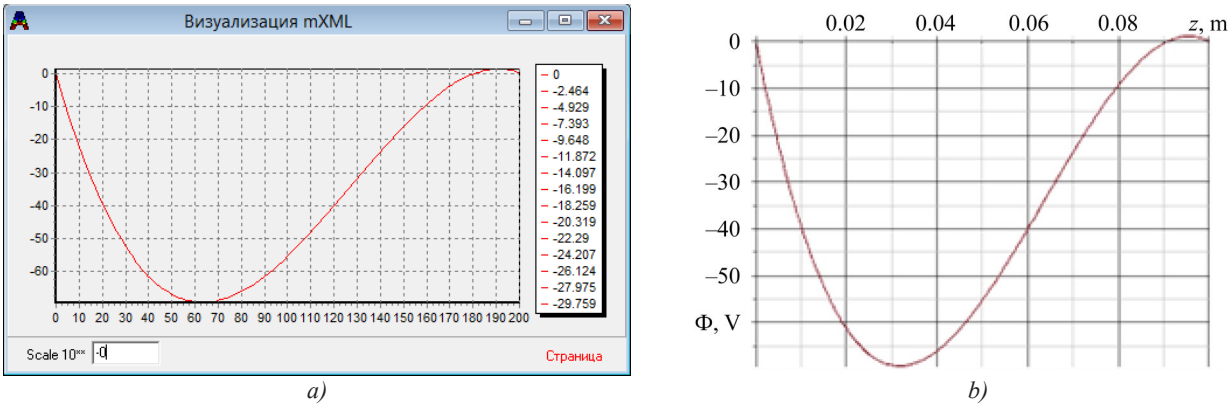

a) *b)*

Fig. 9. Electric potential in the plate: *a* — ACELAN; *b* — applied theory

Discussion. The key result of this research is an applied two-dimensional theory and the demonstration of a high degree of agreement between the solutions obtained from it and the simulation data in the ACELAN finite element package. The deviation in the calculation of the first resonant frequency is only 0.8%, which is more than sufficient for engineering applications. Visual and quantitative comparison of the graphs of deflections, horizontal displacements, and the distribution of electric potential under forced vibrations also shows their almost complete agreement (Figs. 5, 7, 9), which confirms the proposed model adequacy in the frequency range under consideration.

The primary application of the developed theory is the low-frequency range. The structural geometry is thin plates. The range of variation of the material parameters of the layers is relatively small. For wider property ranges, when constructing the applied theory, it will be necessary to take into account the broken normal and use a higher order of approximation for the characteristics of the mechanical and electrical fields across the thickness of the structure.

The proposed theory eliminates resource-intensive 3D modeling at the preliminary design stages. The practical significance of the results is in the creation of an efficient and fast tool for engineers and researchers: instead of time-consuming calculations in "heavy" CAE packages, analytical or numerically analytical solutions of equations (7)–(10) can be used to quickly evaluate dynamic characteristics, conduct parametric studies, and optimize the designs of piezoelectric transducers, sensors, and energy harvesting devices.

Conclusion. Within the framework of the study, the problem of constructing and validating an applied two-dimensional theory for calculating the transverse vibrations of layered plates made of a 1–3 piezocomposite and porous piezoactive 3–0 and 3–3 elements is successfully solved.

A mathematical model based on the Kirchhoff-Love hypothesis is developed to describe the dynamic behavior of a thin layered electroelastic plate with opposing longitudinal polarization of the layers.

A system of differential equations is derived, which, for the particular case of a two-layer panel, reduces to a single equation that admits an analytical solution.

The proposed theory is validated through comparing its results with numerical simulation data in the ACELAN finite element package. The error in determining the first resonant frequency does not exceed 0.8%.

The adequacy of the theory in calculating forced vibrations is proven: the profiles of vertical and horizontal displacements, as well as the distribution of electric potential, calculated using the applied theory, almost completely coincides with the results of finite element modeling.

Thus, it is shown that the proposed two-dimensional theory is an effective and computationally efficient tool for the analysis and design of thin-walled structures made of piezocomposite materials, which allows for a significant acceleration of development compared with the use of universal finite element packages.

Prospects for further research are related to the development of the next level of homogenization — the transition to the efficient properties of a 2–2 composite with subsequent consideration of a two-layer plate — as well as with more complex approximations of mechanical and electrical fields, including consideration of edge effects. However, when complicating the model, it should be remembered that the primary practical purpose of such theories is the calculation of the output integral characteristics of devices: resonant frequencies, output electrical potential, power, etc.

References

1. Newnham RE, Skinner DP, Cross LE. Connectivity and Piezoelectric-Pyroelectric Composites. *Materials Research Bulletin.* 1978;13(5):525–536. https://doi.org/10.1016/0025-5408(78)90161-7

2. Avellaneda M, Swart PJ. Calculating the Performance of 1–3 Piezocomposite for Hydrophone Applications: An Effective Medium Approach. *The Journal of the Acoustical Society of America.* 1998;103(3):1449–1467. http://doi.org/10.1121/1.421306

3. Berger H, Kari S, Gabbert U, Rodriguez-Ramos R, Guinovart-Diaz R, Otero JA, et al. An Analytical and Numerical Approach for Calculating Effective Material Coefficients of Piezoelectric Fiber Composites. *International Journal* of *Solids* and *Structures*. 2005;42(21–22):5692–5714. http://doi.org/10.1016/j.ijsolstr.2005.03.016

4. Bravo-Castillero J, Guinovart-Díaz R, Sabina FJ, Rodríguez-Ramos R. Closed-Form Expressions for the Effective Coefficients of a Fiber-reinforced Composite with Transversely Isotropic Constituents – II. Piezoelectric and Square Symmetry. *Mechanics of Materials.* 2001;33(4):237–248. http://doi.org/10.1016/S0167-6636(00)00060-0

5. Castillero JB, Diaz RG, Hernandez JAO, Ramos RR. Electromechanical Properties of Continuous Fibre-reinforced Piezoelectric Composites. *Mechanics of Composite Materials.* 1997;33:475–482. https://doi.org/10.1007/BF02256903

6. Gibiansky LV, Torquato S. On the Use of Homogenization Theory to Design Optimal Piezocomposites for Hydrophone Applications. *Journal of the Mechanics and Physics of Solids.* 1997;45(5):689–708. https://doi.org/10.1016/S0022-5096(96)00106-8

7. Guinovart-Dıaz R, Bravo-Castillero J, Rodrıguez-Ramos R, Sabina FJ, Martınez-Rosado R. Overall Properties of Piezocomposite Materials 1–3. *Materials Letters.* 2001;48(2):93–98. http://doi.org/10.1016/S0167-577X(00)00285-8

8. Levin VM, Sabina FJ, Bravo-Castillero J, Guinovart-Díaz R, Rodríguez-Ramos R, Valdiviezo-Mijangos OC. Analysis of Effective Properties of Electroelastic Composites Using the Self-Consistent and Asymptotic Homogenization Methods. *International Journal of Engineering Science.* 2008;46(8):818–834. http://doi.org/10.1016/j.ijengsci.2008.01.017

9. Sevostianov I, Levin V, Kachanov M. On the Modeling and Design of Piezocomposites with Prescribed Properties. *Archive of Applied Mechanics.* 2001;71:733–747. http://doi.org/10.1007/s004190100181

10. Pramanik R, Arockiarajan A. Effective Properties and Nonlinearities in 1–3 Piezocomposites: A Comprehensive Review. *Smart Materials and Structures*. 2019;28(10):103001. https://doi.org/10.1088/1361-665X/ab350a

11. Aloui R, Larbi W, Chouchane M. Uncertainty Quantification and Global Sensitivity Analysis of Piezoelectric Energy Harvesting Using Macro Fiber Composites. *Smart Materials* and *Structures*. 2020;29(9):095014. http://doi.org/10.1088/1361-665X/ab9f12

12. Yu Shi, Hallett SR, Meiling Zhu. Energy Harvesting Behaviour for Aircraft Composites Structures Using Macro-Fibre Composite: Part I – Integration and Experiment. *Composite Structures.* 2017;160:1279–1286. https://doi.org/10.1016/j.compstruct.2016.11.037

13. Hyun J Song, Young-Tai Choi, Wereley NM, Purekar A. Comparison of Monolithic and Composite Piezoelectric Material–based Energy Harvesting Devices. *Journal of Intelligent Material Systems and Structures.* 2014;25(14):1825–1837. http://doi.org/10.1177/1045389X14530592

14. Swallow LM, Luo JK, Siores E, Patel I, Dodds D. A Piezoelectric Fibre Composite Based Energy Harvesting Device for Potential Wearable Applications. *Smart Materials* and *Structures*. 2008;17(2):025017. http://doi.org/10.1088/0964-1726/17/2/025017

15. Della CN, Dongwei Shu. Performance of 1–3 Piezoelectric Composites with Porous Piezoelectric Matrix. *Applied Physics Letters*. 2013;103:132905. https://doi.org/10.1063/1.4822109

16. Della ChN, Dongwei Shu. The Performance of 1–3 Piezoelectric Composites with a Porous Non-piezoelectric Matrix. *Acta Materialia.* 2008;56(4):754–761. https://doi.org/10.1016/j.actamat.2007.10.022

17. Gibiansky LV, Torquato S. On the Use of Homogenization Theory to Design Optimal Piezocomposites for Hydrophone Applications. *Journal of the Mechanics and Physics of Solids.* 1997;45(5):689–708. https://doi.org/10.1016/S0022-5096(96)00106-8

18. Sigmund O, Torquato S, Aksay IA. On the Design of 1–3 Piezocomposites Using Topology Optimization. *Journal of Materials Research.* 1998;13:1038–1048. https://doi.org/10.1557/JMR.1998.0145

19. Sladek J, Novak P, Bishay PL, Sladek V. Effective Properties of Cement-based Porous Piezoelectric Ceramic Composites. *Construction and Building Materials.* 2018;190:1208–1214. https://doi.org/10.1016/j.conbuildmat.2018.09.127

20. Nasedkin AV, Oganesyan PA, Soloviev AN. Analysis of Rosen Type Energy Harvesting Devices from Porous Piezoceramics with Great Longitudinal Piezomodulus. *Zeitschrift für Angewandte Mathematik und Mechanik.* 2021;101(3):e202000129. http://doi.org/10.1002/zamm.202000129

21. Roscow JI, Lewis RWC, Taylor J, Bowen CR. Modelling and Fabrication of Porous Sandwich Layer Barium Titanate with Improved Piezoelectric Energy Harvesting Figures of Merit. *Acta Materialia*. 2017;128:207–217. http://doi.org/10.1016/j.actamat.2017.02.029

22. Rybyanets AN, Naumenko AA, Lugovaya MA, Shvetsova NA. Electric Power Generations from PZT Composite and Porous Ceramics for Energy Harvesting Devices. *Ferroelectrics.* 2015;484(1):95–100. https://doi.org/10.1080/00150193.2015.1060065

23. Mingyang Yan, Zhida Xiao, Jingjing Ye, Xi Yuan, Zihe Li, Chris Bowen, et al. Porous Ferroelectric Materials for Energy Technologies: Current Status and Future Perspectives. *Energy & Environmental Science.* 2021;14(12):6158–6190. http://doi.org/10.1039/d1ee03025f

24. Do TB, Nasedkin A, Oganesyan P, Soloviev A. Multilevel Modeling of 1-3 Piezoelectric Energy Harvester Based on Porous Piezoceramics. *Journal of Applied and Computational Mechanics.* 2023;9(3):763–774. http://doi.org/10.22055/jacm.2023.42264.3900

25. Belokon' AV, Nasedkin AV, Solov'ev AN. New Schemes for the Finite-Element Dynamic Analysis of Piezoelectric Devices. *Journal of Applied Mathematics and Mechanics.* 2002;66(3):481–490. http://doi.org/10.1016/S0021-8928(02)00058-8

26. Oganesyan PA, Shtein OO. Implementation of Basic Operations for Sparse Matrices when Solving a Generalized Eigenvalue Problem in the ACELAN-COMPOS Complex. *Advanced Engineering Research (Rostov-on-Don).* 2023;23(2):121–129. https://doi.org/10.23947/2687-1653-2023-23-2-121-129

About the Authors:

Arkadiy N. Soloviev, Dr.Sci. (Phys.-Math.), Professor of the Mathematics and Physics Department, Crimean Engineering and Pedagogical University named after Fevzi Yakubov (8, Uchebnyi Lane, Simferopol, 295015, Republic of Crimea), Chief Researcher of the Research and Production Center for Engineering Technologies, Crimean Engineering and Pedagogical University named after Fevzi Yakubov (8, Uchebnyi Lane, Simferopol, 295015, Republic of Crimea), SPIN-code, ORCID, ScopusID, ResearcherID, solovievarc@gmail.com

Maria S. Germanchuk, Cand.Sci. (Phys.-Math.), Associate Professor of the Informatics Department, V.I. Vernadsky Crimean Federal University (4, Vernadskogo Prospect, Simferopol, 295007, Republic of Crimea), Associate Professor of the Mathematics and Physics Department, Crimean Engineering and Pedagogical University named after Fevzi Yakubov (8, Uchebnyi Lane, Simferopol, 295015, Republic of Crimea**)**, SPIN-code, ORCID, ScopusID, ResearcherID, m.german4uk@yandex.ru

Pavel A. Oganesyan, Cand.Sci. (Phys.-Math.), Associate Professor of the Mathematical Modeling Department, Vorovich Institute for Mathematics, Mechanics, and Computer Science, Southern Federal University (8a, Milchakova Str., Rostov-on-Don, 344058, Russian Federation), SPIN-code, ORCID, ScopusID, poganesyan@sfedu.ru

Claimed Contributorship:

AN Soloviev: conceptualization, supervision, funding acquisition, methodology, writing – original draft preparation, writing – review & editing.

MS Germanchuk: formal analysis, validation, visualization.

PA Oganesyan: investigation, software, funding acquisition, visualization.

***Conflict of Interest Statement*: the authors declare no conflict of interest.**

All authors have read and approved the final version of the manuscript.

Об авторах:

Аркадий Николаевич Соловьев, доктор физико-математических наук, профессор кафедры «Математика и физика» Крымского инженерно-педагогического университета имени Февзи Якубова (295015, Республика Крым, г. Симферополь, пер. Учебный, д. 8), главный научный сотрудник Научно-производственного центра инжиниринговых технологий Крымского инженерно-педагогического университета имени Февзи Якубова (295015, Республика Крым, г. Симферополь, пер. Учебный, д. 8), SPIN-код, ORCID, ScopusID, ResearcherID, solovievarc@gmail.com

Мария Сергеевна Германчук, кандидат физико-математических наук, доцент кафедры «Информатика» Крымского федерального университета им. В.И. Вернадского, (295007, Республика Крым, г. Симферополь, пр. Вернадского, д. 4), SPIN-код, ORCID, ScopusID, ResearcherID, m.german4uk@yandex.ru

Павел Артурович Оганесян, кандидат физико-математических наук, доцент кафедры «Математическое моделирование» Южного федерального университета. (344058 г. Ростов-на-Дону, ул. Мильчакова 8а, ИММиК), SPIN-код, ORCID, ScopusID, poganesyan@sfedu.ru

Заявленный вклад авторов:

А.Н. Соловьев: разработка концепции, научное руководство, получение финансирования, разработка методологии, написание черновика рукописи, написание рукописи — внесение замечаний и исправлений.

М.С. Германчук: формальный анализ, валидация результатов, создание и подготовка рукописи, визуализация.

П.А. Оганесян: проведение исследования, разработка программного обеспечения, получение финансирования, визуализация.

***Конфликт интересов:* авторы заявляют об отсутствии конфликта интересов.**

Все авторы прочитали и одобрили окончательный вариант рукописи.

Received / Поступила в редакцию 01.12.2025
Reviewed / Поступила после рецензирования 18.12.2025
Accepted / Принята к публикации 12.01.2026